Organic & Biomolecular Chemistry

PAPER

View Article Online
View Journal | View Issue

Cite this: *Org. Biomol. Chem.*, 2015, **13**, 10205

Benzyl anion transfer in the fragmentation of *N*-(phenylsulfonyl)-benzeneacetamides: a gas-phase intramolecular S_NAr reaction†

Shanshan Shen,[a] Yunfeng Chai,[b] Yaqin Liu,[a] Chang Li[b] and Yuanjiang Pan*[a]

Received 30th July 2015,
Accepted 18th August 2015

DOI: 10.1039/c5ob01582k

www.rsc.org/obc

In this study, we report a gas-phase benzyl anion transfer *via* intramolecular aromatic nucleophilic substitution (S_NAr) during the course of tandem mass spectrometry of deprotonated *N*-(phenylsulfonyl)-benzeneacetamide. Upon collisional activation, the formation of the initial ion/neutral complex ($[C_6H_5CH_2^-/C_6H_5SO_2NCO]$), which was generated by heterolytic cleavage of the CH_2–CO bond, is proposed as the key step. Subsequently, the anionic counterpart, benzyl anion, is transferred to conduct the intra-complex S_NAr reaction. After losing neutral HNCO, the intermediate gives rise to product ion **B** at *m*/*z* 231, whose structure is confirmed by comparing the multistage spectra with those of deprotonated 2-benzylbenzenesulfinic acid and (benzylsulfonyl)benzene. In addition, intra-complex proton transfer is also observed within the complex $[C_6H_5CH_2^-/C_6H_5SO_2NCO]$ to generate product ion **C** at *m*/*z* 182. The INC-mediated mechanism was corroborated by theoretical calculations, isotope experiments, breakdown curve, substituent experiments, *etc*. This work may provide further understanding of the physicochemical properties of the gaseous benzyl anion.

Introduction

Carbanions are highly-reactive intermediates in numerous chemical processes and widely employed in organic solution reactions.[1] In the condensed phase, they are usually paired with the corresponding metal counterions to form organometallics. Evaluation of their intrinsic reactivity is quite a big challenge because they are quite sensitive to temperature, additives and solvent.[2,3] Therefore, it is of great importance and general interest to gain insight into the essential behavior of monomeric carbanions in the gas phase.

Mass spectrometry (MS) has become an indispensable tool in conducting fundamental studies of gas-phase ion chemistry.[4–7] In gaseous ionic reactions, ion-neutral complex (INC) intermediates are extensively invoked to rationalize the generation of some special product ions.[8–12] Previously, numerous theoretical and experimental studies have been reported on the existence and importance of INC in unimolecular dissociation reactions in MS.[13,14] An INC consists of an ionic fragment and a neutral counterpart which bind together through electrostatic attraction but still maintain its individual mobility. In such a temporary system, various intriguing chemical reactions occur prior to final separation of the INC partners. Among them, the most common INC-mediated process is proton transfer.[13] Several other transfer reactions were also observed including transacylation,[15] hydride transfer,[16–19] electron transfer,[20,21] benzyl cation transfer (BCT),[22–24] *etc*. Particularly, research on intramolecular BCT has been well-documented and has received considerable interest. In contrast, quite a few studies were focused on the transfer of carbanions, as the occurrence of such reactions requires a suitable carbanion donor and acceptor. In many cases, however, most compounds analyzed by negative-ion MS contain one or several basic sites which can easily capture a carbocation, and thus, carbanion transfer is usually inhibited by other competing reactions.

The benzyl anion, the simplest aromatic negative ion containing an exocyclic carbon atom and a highly-reactive intermediate in various chemical and biochemical reactions,[25–27] is less fragile than alkyl types of carbanions due to resonance stabilization.[28] Efforts have been made to obtain its crystal structure under low temperature and strictly anhydrous conditions, but failed due to its rapid decomposition.[29] By contrast, the benzyl anion is relatively stable in the gas phase, and thus can be obtained in the collision induced dissociation (CID) process of some specific precursor ions in MS. The

[a]*Department of Chemistry, Zhejiang University, Hangzhou 310027, China. E-mail: panyuanjiang@zju.edu.cn; Fax: +86-571-87951629; Tel: +86-571-87951264*
[b]*College of Pharmaceutical Sciences, Zhejiang University, Hangzhou 310058, China*
†Electronic supplementary information (ESI) available: NMR spectra of model compounds, Cartesian coordinates, total energies, zero point energy corrections and the number of imaginary frequencies of the structures discussed in the text. See DOI: 10.1039/c5ob01582k

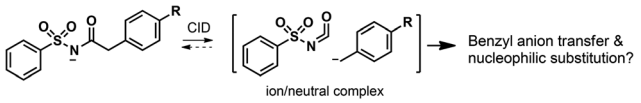

Scheme 1 Gas-phase generation of the ion/neutral complex containing the reactants through the collision-induced dissociation (CID) method.

benzyl anion is so highly electron-rich that it can act as an electron donor to undergo a single electron transfer reaction.[20] It is also an ideal Brønsted base as it is able to capture a proton from an aromatic ring.[30] In view of its well-known nucleophilicity, here we question if it could undergo intramolecular transfer to achieve gas-phase nucleophilic substitution reactions.

The motivation of the present investigation is to delve into the gas-phase benzyl anion transfer (BAT) reaction *via* INC, which is not only essentially important for gas-phase ionic reactions, but also crucial in expanding our understanding on the chemical nature of the benzyl anion. Therefore, we selected *N*-(phenylsulfonyl)-benzeneacetamides as the model. Presumably, the deprotonated model compounds can simultaneously *in situ* generate both the nucleophile (benzyl anion) and the electrophilic species (benzenesulfonyl isocyanate moiety) (Scheme 1) in tandem mass spectrometry.

Experimental

Mass spectrometry

The samples were analyzed with negative ion ESI-MS on a Bruker Esquire 3000^{plus} ion trap mass spectrometer (Bruker-Franzen Analytik GmbH, Bremen, Germany), with data acquisition using the Esquire 5.0 software. The compounds were dissolved in methanol, and then the solutions were infused into the source chamber at a flow rate of 3 μL min^{-1}. Nitrogen was used as the nebulizing gas at a pressure of 10 psi, and the drying gas at a flow rate of 5 L min^{-1}. The capillary voltage was set at 4000 V, and the ion source temperature was set at 250 °C. CID mass spectra were obtained with helium as the collision gas, and the collision energy was set at appropriate collision energies to give energy for dissociation of all samples.

High-resolution mass spectrometry experiments were conducted by using a TripleTOF4600 system with a DuoSpray™ ion source operating in the positive ESI mode (AB SCIEX, CA, USA). The APCI probe of the source was used for fully automatic mass calibration using a Calibrant Delivery System. CDS injects a calibration solution matching the polarity of ionization and calibrates the mass axis of the TripleTOF system in all scan functions used (MS or MS/MS). Data acquisition and processing were carried out using Analyst TF 1.6 and PeakView (AB SCIEX, Foster City, CA) software version 1.2 with the XIC Manager. Solutions were infused from the ESI source at 10 μL min^{-1} with the following parameters applied: ion spray voltage floating (ISVF), 5500 V; temperature, 550 °C; curtain gas, 25 psi; and ion source gas (GS1 and GS2) at 40 psi. The collision energy (CE) was 40 eV, and the collision energy spread (CES) was 15 eV in the MS/MS experiments.

Theoretical calculation

Theoretical calculations were carried out using the Gaussian 03 package of programs.[31] All structures were optimized at the B3LYP/6-31++G(d, p) level of density functional theory (DFT), and were identified as the true minima by the absence of imaginary frequencies. Transition states were identified by the presence of only one imaginary frequency. The minima connected by a given transition structure were confirmed by intrinsic reaction coordinate (IRC) calculations. The energies discussed here are the sum of electronic and thermal energies.

Sample synthesis and preparation

The *N*-(phenylsulfonyl)-benzeneacetamide derivatives (**1–8**) were synthesized from the corresponding phenylacetic acids and benzenesulfonamide in the presence of EDCI and DMAP.[32] Compounds **9–11** were prepared using the corresponding sulfonyl chlorides and 2-phenylacetamide.[33] Deuteration (**8**) and 2-benzylbenzenesulfinic acid (**12**) were obtained following the reported procedures.[34,35] Experimental details, high-resolution mass spectrometry (Table S1†) and ^{1}H NMR data are available in the ESI.† The structure of the representative model compound (**1**) was confirmed by NMR spectroscopy. *N*-(Phenylsulfonyl)-benzeneacetamide (**1**), ^{1}H NMR (600 MHz, DMSO-d_6): δ (ppm) 7.95 (d, 2H), 7.68 (t, 1H), 7.60 (t, 2H), 7.29–7.17 (m, 5H), 3.59 (s, 2H); ^{13}C NMR (150 MHz, DMSO-d_6): δ (ppm) 172.6, 142.3, 137.0, 136.7, 132.3, 132.2, 131.4, 130.6, 130.0, 45.2 (ESI Fig. S4†).

The samples except for compound **8** were dissolved in methanol first, and then diluted with methanol–water (1 : 1, v/v) containing 0.1% ammonia before being introduced into mass spectrometers. Compound **8** was dissolved in methanol-d_4 first, and then diluted with methanol-d_4 before being introduced into the mass spectrometer.

Results and discussion

The gas-phase BAT reaction was explored by investigating the fragmentation pattern of the deprotonated *N*-(phenylsulfonyl)-benzeneacetamides (compounds **1–7**, Fig. 1). Generally, these analogues produced similar fragment ions in the negative

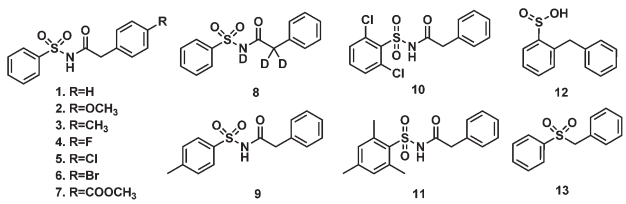

Fig. 1 Compounds for gas-phase benzyl anion transfer studies.

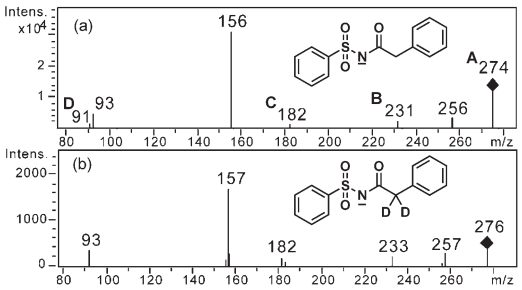

Fig. 2 CID spectra (a) deprotonated compound **1** and (b) dedeuterated compound (**8**). Signal peaks marked with rhombus correspond to the parent ions.

Table 1 CID mass spectral data of the deprotonated *N*-(phenylsulfonyl)-benzeneacetamide derivatives (fragmentation amplitude, 0.8 volts)[a]

No.	R	$[M-H]^-$ *m/z*	**D** $RC_6H_4CH_2^-$	**C** $C_6H_4SO_2NCO^-$	**B** $[(M-H)\text{-}43]^-$
1	–H	274	91 (0.42)[b]	182 (0.67)	231 (2.0)
2	$-OCH_3$	304	121 (0.081)	182 (2.8)	261 (3.9)
3	$-CH_3$	288	105 (0.12)	182 (1.4)	245 (2.6)
4	–F	292	109 (0.37)	182 (0.94)	249 (3.0)
5	$-^{35}Cl$	308	125 (8.8)	182 (1.4)	265 (8.7)
6	$-^{79}Br$	352	169 (9.8)	182 (1.2)	309 (7.0)
7	$-COOCH_3$	332	149 (100)	N. D.[c]	289 (1.1)

[a] For other ions, see the CID spectra in Fig. S1 (ESI). [b] *m/z* (Relative abundance %, related to the base peak). [c] N. D.: not detected.

ESI-MS/MS experiments but in different relative abundances. A typical CID spectrum for the $[M-H]^-$ ion of compound **1** is shown in Fig. 2a; partial CID MS data are summarized in Table 1.

For clarification, compound **1** was picked up to exemplify the characteristic fragmentations. On the basis of exhaustive investigations of gaseous negative ions,[36,37] we propose the fragmentation routes of some selected product ions generated from deprotonated compound **1** as depicted in Scheme 2. After deprotonation, the $[M-H]^-$ ion may form different isomers, as the methylene proton may undergo migration. Among these, **A-1** should possess higher population, which can be confirmed by theoretical calculation results that the

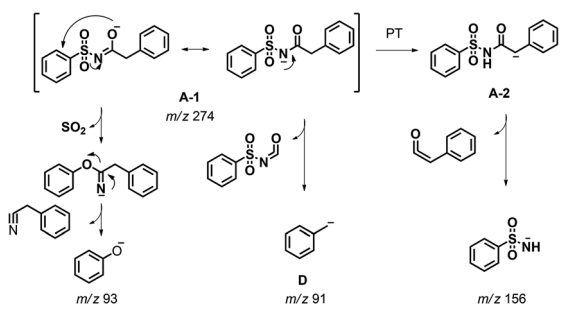

Scheme 2 Proposed MS/MS fragmentation mechanisms for the selected product ions from deprotonated compound **1**.

total energy of the isomer **A-1** is 21.8 kcal mol^{-1} lower than that of **A-2**. As for the two mesomeric structures of **A-1**, they are likely to share similar proportions because calculational results reveal close charge distributions of nitrogen (−0.407) and oxygen (−0.461) (Fig. S2†). The most abundant ion at *m/z* 156 is attributed to the (phenylsulfonyl)amide anion, originating from the heterolytic cleavage of the acylamide bond of **A-2**. The fragment ion at *m/z* 93 is assigned as the phenolate anion, derived from Smiles rearrangement from **A-1** *via* the stepwise loss of SO_2 and $C_6H_5CH_2CN$. Such cases are not unusual in the gas-phase anionic fragmentations.[38–40] Several other common fragmentations were also observed, such as the ion at *m/z* 256 that results from the loss of H_2O, and the benzyl anion at *m/z* 91 that results from the direct decomposition of **A-1**. Herein, the other two product ions, *m/z* 182 (**C**) and *m/z* 231 (**B**), drew our interest on their generation pathways since they can't be explained by conventional mechanisms.

Benzyl anion transfer within INC

The recognizable product ion **B** (*m/z* 231) of interest is formed by elimination of 43 Da (Fig. 2a). The accurate mass of the fragment ion, 231.0482, corresponding to $C_{13}H_{11}O_2S$ (calculated mass = 231.0485), indicates that the expelled neutral is CHON, likely isocyanic acid. Although such a loss appears trivial, the mechanism is not straightforward since the deprotonated molecule should undergo a complicated skeletal rearrangement to eliminate HNCO.

The structure of **B** was confirmed by multistage mass spectrometry (Fig. 3). Two comparative ions with definite structures of $C_6H_5CH_2C_6H_4SO_2^-$ or $C_6H_5(CH^-)SO_2C_6H_5$ were generated from deprotonated 2-benzylbenzenesulfinic acid (**12**, Fig. 1) and (benzylsulfonyl)benzene (**13**) respectively, and subsequently subjected to collisional dissociation. The fragmentation pattern of ion **B** is almost the same as that of

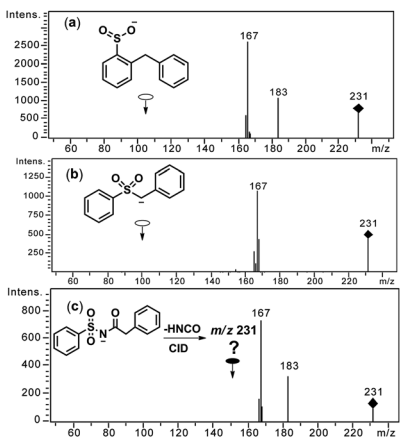

Fig. 3 CID spectra of the ion at *m/z* 231 derived from (a) deprotonated 2-benzylbenzenesulfinic acid (**12**), (b) deprotonated (benzylsulfonyl)-benzene (**13**), and (c) the loss of HNCO from deprotonated **1**. Signal peaks marked with rhombus correspond to the parent ions.

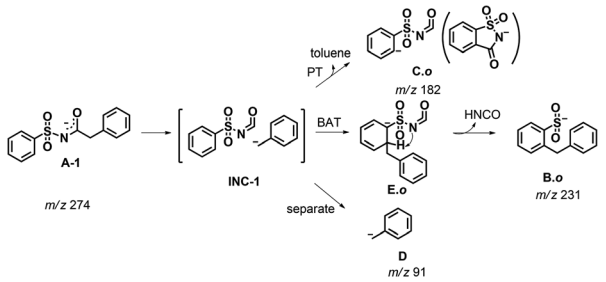

Scheme 3 Gas-phase fragmentation reaction mechanisms proposed for the INC-involved product ions from deprotonated compound **1**; *ortho*-position selected as an example for clear illustration; the italic suffix represents the reaction position of the phenyl ring.

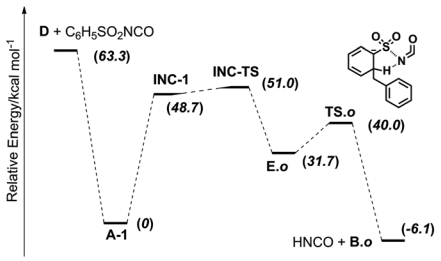

Fig. 4 DFT energy diagram for the S_NAr reaction between $C_6H_5CH_2^-$ (**D**) and $C_6H_5SO_2NCO$. All structures were optimized at the B3LYP/6-31++G(d,p) level of theory in kcal mol^{-1} (in parentheses).

deprotonated **12** but differs from that of deprotonated **13**, which gives us a vital clue to its generation mechanism.

As aforementioned, the anticipative way to commence this investigation is to consider the widespread INC mechanistic scenario as the route exhibited in Scheme 3. Given the fact that the benzyl anion is electron-rich while the neutral aromatic moiety is highly electron-deficient, the nucleophilic attack of benzyl carbanion at the phenyl ring can easily occur to form an anionic σ-complex.[41] This marked BAT achieves the S_NAr reaction between the benzyl anion and the phenyl ring, and successively activates the corresponding ring hydrogen to become mobile. Once the hydrogen is attached on the dissociative isocyanic nitrogen, the elimination of isocyanic acid occurs to give rise to ion **B.*o***.

Another plausible reaction pathway (**Path 2**) for the loss of HNCO was proposed *via* a three-step process (Scheme 4): incipient cyclisation through the nucleophilic attack of the benzylic anion at the phenyl ring forms a six-membered ring, and subsequent HNCO loss gives rise to the product ion. At first glance, **Path 2** is of faint chance because it is conformationally unfavourable for a saturated carbon to adopt an extra hydrogen in the hydrogen transfer step.

To verify the foregoing speculation, compound **8** was synthesized to check the possibility of the two proposed pathways since they will generate two different product ions with different *m*/*z* values. Specifically, if the reaction underwent the cyclisation channel (**Path 2**), a loss of DNCO would be expected to give the product ion at *m*/*z* 232; on the contrary, if BAT takes place (INC-pathway), the loss of HNCO from the intermediate will generate a product ion at *m*/*z* 233. Consequently, the two mechanisms can be readily distinguished from one another. According to the ESI-MS/MS spectrum of the $[M - D]^-$ ion of compound **8** (Fig. 2b), the product ion at *m*/*z* 233 was observed rather than *m*/*z* 232, which experimentally corroborates the possibility of the INC-pathway.

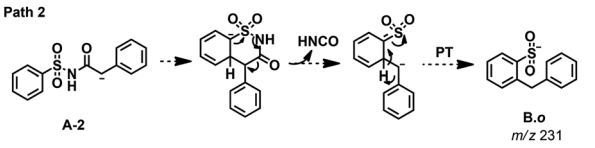

Scheme 4 Plausible MS/MS fragmentation mechanism for the loss of HNCO from the cyclization reaction.

What's more, DFT calculations were conducted at the B3LYP/6-31++G(d, p) level of theory to further confirm the mechanism of the present INC-mediated BAT reaction. Compound **1** is used as a representative example. An energy diagram was created as illustrated in Fig. 4, and full details of the structures and energies of involved species are given in the ESI.† The INC (**INC-1**), formed by dissociation of the parent ion (**A-1**), is located 14.6 kcal mol^{-1} below the separated $C_6H_5CH_2^-$ (**D**) and $C_6H_5SO_2NCO$. Within **INC-1**, the benzyl anion undergoes aromatic nucleophilic attack at the *ortho* site of $C_6H_5SO_2NCO$ to form a much more stable anionic σ-complex, **E.*o***, in which the calculated C_{aryl}–C bond length is 1.58 Å. The conversion of **INC-1** to **E.*o*** is almost barrierless with a relatively low energy barrier (**INC-TS**) being only 2.3 kcal mol^{-1} higher than that of **INC-1** (see ESI Fig. S4† for more details). The subsequent loss of HNCO is thermodynamically favourable since the total energy of the products is 37.8 kcal mol^{-1} lower than that of **E.*o***, with a not very high energy barrier (**TS.*o***) to be surmounted. It should be noted that the last step might be triggered by the dissociative isocyanate anion on account of the overwhelming tendency towards the cleavage of the scissile S–N bond (1.94 Å). The theoretical calculations provide reasonable and reliable evidence for the S_NAr reaction between $C_6H_5CH_2^-$ and $C_6H_5SO_2NCO$ involving a multistep addition–elimination pathway through an anionic σ-complex intermediate.

Proton transfer within INC

The other interesting product ion **C** (*m*/*z* 182), corresponding to the elimination of toluene, is derived from intra-complex proton transfer (PT) attributing to the Brønsted basicity of the benzyl anion. As proposed in the upper reaction route in Scheme 3, within **INC-1**, the benzyl anion captures an *ortho* proton from the neutral counterpart leading to the formation of **C.*o***. This route is similar to that discussed by Lu *et al.*[30] On the other hand, calculations show that the product ion **C.*o***, resulting from the *ortho*-channel, stabilizes the negative charge by cyclization (as shown in parentheses), whereby it is placed in an extremely deep potential well compared with the *meta*-

or *para*-channel (ESI Fig. S3†). Previous gas-phase kinetic studies have explained the reason why the product ion exhibited such a low intensity signal. That is, proton transfer to charge-delocalized anions proceeds with low efficiency even when energetically favorable.[42]

Breakdown curve

Supporting evidence for the existence of INC is obtained from CID experiments at varying energies. The breakdown graph for deprotonated **1**, shown in Fig. 5, indicates that, with increasing collision energy, the sum of the abundance of the INC-involved product ions, **C** and **B**, keeps decreasing after reaching the maximum at 0.82 volts; a steady increase is observed for one of their rival ions, **D** (*m*/*z* 91). This is the behavior one would expect[43,44] for an INC-mediated reaction since the stability of an INC is quite susceptible to collision energy.

Substituent effect

Substituent effects are very helpful in probing different reaction mechanisms.[45–47] As shown in Scheme 3, the INC can generate three product ions, **B**, **C** and **D**. The relative abundances of these competing ions highly depend on the presence of substituents on the benzyl ring which alter either the stability of the product ions or the reactivity of the intermediates. Specifically, an electron-withdrawing substituent (EWS) is able to stabilize the benzyl anion (**D**) by spreading the negative charge. In contrast, an electron-donating substituent (EDS) increases both the Brønsted basicity and nucleophilicity of the benzylic anion, resulting in stronger reactivity towards the PT route or the S_NAr route, respectively. In a word, the former is expected to promote the formation of product ion **D**, while the latter is expected to prefer the generation of **B** and **C**.

A series of compounds bearing different substituents at the *para*-site of the phenylacetyl moiety (Fig. 1) were studied systematically to further understand the reaction mechanism. All the compounds exhibit similar fragmentation patterns as stated above, whereas the relative intensities of the three competitive INC-product ions (**B**, **C** and **D**) vary significantly as the substituent changes (Table 1). As depicted in Fig. 6, the intensity ratio of these three product ions (**D** over (**B** + **C**)) generally follows a linear relationship with the Hammett substituent

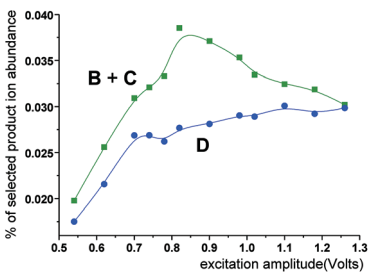

Fig. 5 Breakdown graph for the selected product ions of deprotonated **1**.

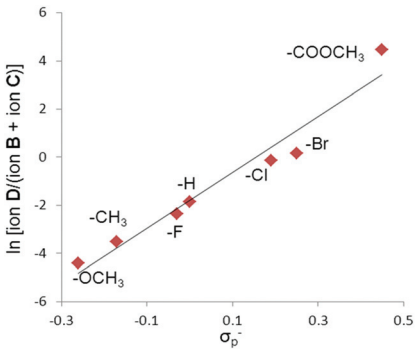

Fig. 6 Competition between benzyl anion formation (ion **D**) and INC-mediated PT & BAT (ion **C** + ion **B**) from the $[M - H]^-$ ions of *N*-(phenylsulfonyl)-benzeneacetamides with different substituents.

constant σ_p^-.[48] The results can strongly support our proposed INC-mediated mechanism.

Blocking experiments

It is well known that S_NAr is accelerated by electron-withdrawing groups, especially at positions *ortho* and *para* to the leaving group. Last but not least, CID spectra of deprotonated 2-phenyl-*N*-tosylacetamide (**9**), *N*-((2,6-dichlorophenyl)sulfonyl)-2-phenylacetamide (**10**) and *N*-(mesitylsulfonyl)-2-phenylacetamide (**11**) were studied (Fig. 7), confirming the reaction position of BAT where the signal peak assigned to the loss of HNCO is what we focus on.

As shown in Fig. 7, the results turned out to be in good accordance with the criterion. When the two *ortho* sites (Fig. 7b) or both the *ortho* and *para* sites (Fig. 7c) are occupied, no signal peak corresponding to the loss of HNCO is observed; whereas, in the case of the *para*-blocked one, the abundance of the target peak (*m*/*z* 245, Fig. 7a) decreases (RA, 0.93%) com-

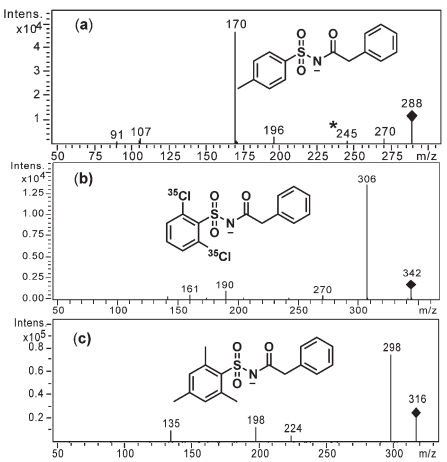

Fig. 7 CID mass spectra of deprotonated (a) 2-phenyl-*N*-tosylacetamide (**9**), (b) *N*-((2,6-dichlorophenyl)sulfonyl)-2-phenylacetamide (**10**) and (c) *N*-(mesitylsulfonyl)-2-phenylacetamide (**11**). The signal peak corresponding to HNCO loss is marked with asterisks for clarity.

pared with the unsubstituted case, but is still legible. The blocking-experiment results reveal that the two *ortho*s are the most likely positions that the benzyl anion attacks. The foregoing results are in accord with the orientation effect and reactivity in S_NAr.

In addition, in the *ortho*-blocked case (**10**), no loss of toluene was observed (Fig. 7b), which suggests that an *ortho* hydrogen is mostly inclined to be transferred to generate product ion **C**. The other two cases (**9**, **11**) are not applicable for the site-determination of PT because the benzylic protons of the methyl substituent may participate in the PT process.[23]

Conclusions

We have investigated the interesting gas-phase benzyl anion transfer reaction in the fragmentation of deprotonated *N*-(phenylsulfonyl)-benzeneacetamides by means of tandem mass spectrometry. The key step of the transfer reaction was supposed to be the formation of the complex [$RC_6H_4CH_2^-$/$C_6H_5SO_2NCO$], which was confirmed by comprehensive experimental and theoretical evidence. In addition, the BAT process was validated to be aromatic nucleophilic substitution in which the benzyl anions act as nucleophiles. The present work can help us further understand gaseous nucleophilicity of the benzyl anion and expand the scope of INC-involved gas-phase reactions.

Acknowledgements

The authors gratefully acknowledge financial support from the National Natural Science Foundation of China (no. 21327010).

Notes and references

1 R. Bates and C. A. Ogle, *Carbanion Chemistry*, Springer-Verlag, Berlin, 1983.
2 M. Smith and J. March, *March's Advanced Organic Chemistry: Reactions, Mechanisms, and Structure*, John Wiley & Sons, Inc., 605 Third Avenue, New York, 2001.
3 Z. X. Tian and S. R. Kass, *Chem. Rev.*, 2013, **113**(9), 6986.
4 C. Lifshitz, *Chem. Soc. Rev.*, 2001, **30**(3), 186.
5 L. Operti and R. Rabezzana, *Mass Spectrom. Rev.*, 2006, **25**(3), 483.
6 C. Lifshitz, *Int. Rev. Phys. Chem.*, 1987, **6**(1), 35.
7 S. K. Kim, T. Ha and J. P. Schermann, *Phys. Chem. Chem. Phys.*, 2010, **12**(41), 13366.
8 M. Edelson-Averbukh and A. Mandelbaum, *J. Chem. Soc., Perkin Trans. 2*, 2000, **5**, 989.
9 S. S. Shen, Y. F. Chai, G. F. Weng and Y. J. Pan, *J. Am. Soc. Mass Spectrom.*, 2014, **25**(9), 1662.
10 C. Guo, K. Z. Jiang, L. Yue, Z. M. Xia, X. X. Wang and Y. J. Pan, *Org. Biomol. Chem.*, 2012, **10**(35), 7070.
11 J. Bialecki, J. Ruzicka and A. B. Attygalle, *J. Mass Spectrom.*, 2006, **41**(9), 1195.
12 C. Matthias and D. Kuck, *Croat. Chem. Acta*, 2009, **82**(1), 7.
13 R. D. Bowen, *Acc. Chem. Res.*, 1991, **24**(12), 364.
14 P. Longevialle, *Mass Spectrom. Rev.*, 1992, **11**(3), 157.
15 Y. P. Tu, Y. Huang, C. Atsriku, Y. You and J. Cunniff, *Rapid Commun. Mass Spectrom.*, 2009, **23**(13), 1970.
16 M. E. Crestoni, S. Fornarini, M. Lentini and M. Speranza, *J. Phys. Chem.*, 1996, **100**(20), 8285.
17 E. L. Oiestad and E. Uggerud, *Int. J. Mass Spectrom.*, 2000, **199**(1–3), 91–105.
18 H. E. Audier, F. Dahhani, A. Milliet and D. Kuck, *Chem. Commun.*, 1997, 429.
19 C. Matthias, K. Weniger and D. Kuck, *Eur. Mass Spectrom.*, 1995, **1**(5), 445.
20 Y. F. Chai, S. F. Gan and Y. J. Pan, *Acta Chim. Sin.*, 2012, **70**(17), 1805.
21 N. Hu, Y. P. Tu, K. Z. Jiang and Y. J. Pan, *J. Org. Chem.*, 2010, **75**(12), 4244.
22 H. Z. Sun, Y. F. Chai and Y. J. Pan, *J. Org. Chem.*, 2012, **77**(16), 7098.
23 Y. F. Chai, L. Wang, H. Z. Sun, C. Guo and Y. J. Pan, *J. Am. Soc. Mass Spectrom.*, 2012, **23**(5), 823.
24 C. Guo, L. Yue, M. Z. Guo, K. Z. Jiang and Y. J. Pan, *J. Am. Soc. Mass Spectrom.*, 2013, **24**(3), 381.
25 T. P. Begley and S. E. Ealick, *Curr. Opin. Chem. Biol.*, 2004, **8**(5), 508.
26 J. D. Cowan, *Nature*, 1967, **213**(5073), 237.
27 J. P. Richard, T. L. Amyes and M. M. Toteva, *Acc. Chem. Res.*, 2001, **34**(12), 981.
28 B. Bockrath and L. M. Dorfman, *J. Am. Chem. Soc.*, 1974, **96**(18), 5708.
29 M. M. Olmstead and P. P. Power, *J. Am. Chem. Soc.*, 1985, **107**(7), 2174.
30 Z. H. Lu, Y. F. Chai, J. C. Wang, Y. J. Pan, C. R. Sun and S. Zeng, *Rapid Commun. Mass Spectrom.*, 2014, **28**(15), 1641.
31 M. J. Frisch, G. W. Trucks, H. B. Schlegel, G. E. Scuseria, M. A. Robb, J. R. Cheeseman, V. G. Zakrzewski, J. A. Montgomery, R. E. Stratmann, J. C. Burant, S. Dapprich, J. M. Millam, A. D. Daniels, K. N. Kudin, M. C. Strain, O. Farkas, J. Tomasi, V. Barone, M. Cossi, R. Cammi, B. Mennucci, C. Pomelli, C. Adamo, S. Clifford, J. Ochterski, G. A. Petersson, P. Y. Ayala, Q. Cui, K. Morokuma, D. K. Malick, A. D. Rabuck, K. Raghavachari, J. B. Foresman, J. Cioslowski, J. V. Ortiz, B. B. Stefanov, G. Liu, A. Liashenko, P. Piskorz, I. Komaromi, R. Gomperts, R. L. Martin, D. J. Fox, T. Keith, M. A. Al-Laham, C. Y. Peng, A. Nanayakkara, C. Gonzalez, M. Challacombe, P. M. W. Gill, B. Johnson, W. Chen, M. W. Wong, J. L. Andres, C. Gonzalez, M. E. Head-Gordon, S. Replogle and J. A. Pople, *Gaussian 03*, Gaussian, Inc., Pittsburgh, PA, 2003.
32 Y. Luo, Y. Li, K. M. Qiu, X. Lu, J. Fu and H. L. Zhu, *Bioorg. Med. Chem.*, 2011, **19**(20), 6069.
33 Y. H. Jhan, T. W. Kang and J. C. Hsieh, *Tetrahedron Lett.*, 2013, **54**(9), 1155.

34 J. I. G. Cadogan, S. H. Hutchinson and H. McNab, *J. Chem. Soc., Perkin Trans. 1*, 1988, 2875.
35 T. Kamiyama, S. Enomoto and M. Inoue, *Chem. Pharm. Bull.*, 1988, **36**(7), 2652.
36 J. H. Bowie, *Mass Spectrom. Rev.*, 1984, **3**(2), 161.
37 J. H. Bowie, *Mass Spectrom. Rev.*, 1990, **9**(3), 349.
38 Y. P. Zhou, Y. J. Pan, X. J. Cao, J. Wu and K. Z. Jiang, *J. Am. Soc. Mass Spectrom.*, 2007, **18**(10), 1813.
39 N. Hu, P. Y. Liu, K. Z. Jiang, Y. P. Zhou and Y. J. Pan, *Rapid Commun. Mass Spectrom.*, 2008, **22**(17), 2715.
40 T. F. Wang, N. M. M. Nibbering and J. H. Bowie, *Org. Biomol. Chem.*, 2010, **8**(18), 4080.
41 M. Makosza, *Chem. Soc. Rev.*, 2010, **39**(8), 2855.
42 C. C. Han and J. I. Brauman, *J. Am. Chem. Soc.*, 1989, **111**(17), 6491.
43 D. J. McAdoo, *Mass Spectrom. Rev.*, 1988, **7**(4), 363.
44 A. G. Harrison and J. Y. Wang, *Int. J. Mass Spectrom. Ion Processes*, 1997, **160**(1–3), 157.
45 N. Hu, Y. P. Tu, Y. Q. Liu, K. Z. Jiang and Y. J. Pan, *J. Org. Chem.*, 2008, **73**(9), 3369.
46 Y. F. Chai, C. Guo, K. Z. Jiang, Y. J. Pan and C. R. Sun, *Org. Biomol. Chem.*, 2012, **10**(4), 791.
47 L. Bache-Andreassen and E. Uggerud, *Org. Biomol. Chem.*, 2003, **1**(4), 705.
48 C. Hansch, A. Leo and R. W. Taft, *Chem. Rev.*, 1991, **91**(2), 165.